equation

$$\chi_p = \tfrac{1}{3}(\chi_{||} + 2\chi_{\perp}), \qquad (5.26)$$

and this curve is also drawn in Fig. 4. We see that the theory does, indeed, indicate a change in the slope, albeit, not quite so sharp as that seen by Fehrenbach.[24] For $0.3 < 1/y < 1.6$ the powder curve does follow to a good approximation a Curie-Weiss law (with negative Θ). Also, for $1/y > 2.2$ the curve also obeys a Curie-Weiss law, but now with positive Θ. If we extend these two linear regions we may equate the value of T at the point of intersection with the temperature ($\doteq 410°K$) which Fehrenbach finds for the sudden change of slope.

---

[24] C. Fehrenbach, J. Phys. Radium 8, 11 (1937).

The required point is

$$1/y = -kT/\lambda' = 1.80,$$

which gives $\lambda' = -158$ cm^{-1} or, taking $k=0.9$, a value of $\lambda = -176$ cm^{-1}.

Using this value for the spin orbit coupling constant in $CoCl_2$ (assuming, therefore, that this quantity has approximately the same value for $CoCl_2$ as for Co^{++} in $CdCl_2$) we may now evaluate $1/\chi$ as a function of temperature for the concentrated salt. The results are shown in Fig. 5 together with the experimental curves of Bizette et al.[3] We see that the agreement between theory and experiment is quite good for both $\chi_{||}$ and $\chi_{\perp}$.

Structure of the F Center in NaF†

WILLIAM T. DOYLE

Physics Department, Dartmouth College, Hanover, New Hampshire

(Received 13 March 1963)

The electron-nuclear double resonance (ENDOR) method is applied to the study of the structure of the F center in NaF. Hyperfine interactions between the F-center electron and a number of the surrounding nuclear shells are presented and compared with the results of earlier experiments and with theory. It is found that the resolved hyperfine structure is not due to the predominance of the first-shell interaction, as has been thought, but it arises from the fortuitous equality of the first- and second-shell isotropic hyperfine interactions. Electron paramagnetic resonance (EPR) absorption measurements of the resolved structure confirms an expected 31-line resolved pattern. The exceptional resolution found in the ENDOR spectrum permits the identification of interactions with nuclei well beyond the eighth shell. Although the samples also contained large numbers of M centers, no evidence for a paramagnetic M center was found in either the EPR or ENDOR spectra.

I. INTRODUCTION

THE shape of electron paramagnetic resonance (EPR) lines due to F centers in alkali halide crystals arises from hyperfine interactions between the F-center electron and the surrounding nuclei.[1] Although F centers typically exhibit a single broad Gaussian EPR line, in a few crystals, viz., LiF,[2,3] NaF,[2,3] NaH,[4] RbCl,[5] and CsCl,[6] a resolved spectrum has been observed. Rather special relations must obtain among the hyperfine interactions for a resolved spectrum to appear. The simplest case arises when the isotropic interaction with the first shell predominates. Then, if the spin of the first-shell nuclei is $\tfrac{3}{2}$, one expects a nineteen-line

spectrum with a distribution of intensities of 1, 6, 21, 56, 120, 216, 336, 456, 546, and 580, corresponding to total shell nuclear magnetic quantum numbers of ± 9, $\cdots$, 0, respectively.[1] This simple nineteen-line spectrum has been reported in LiF,[2,3] NaF,[2-4,7] and NaH.[4,8] In LiF, however, it is now known that the resolved structure is considerably more complicated. Many more than nineteen lines are observed and the pattern depends strongly upon the orientation of the crystal in the external magnetic field.[7,9,10] In some crystal orientations,[9] and in powdered samples,[4] the resolved structure is obliterated. Electron-nuclear double resonance (ENDOR)[11] studies have shown that in LiF the resolved structure is due to both isotropic and anisotropic hyperfine interactions with the first two nuclear shells[7,10,12]; interactions with all other shells being small

---

[1] A. F. Kip, C. Kittel, R. A. Levy, and A. M. Portis, Phys. Rev. 91, 1066 (1953).
[2] N. Lord, Phys. Rev. 105, 756 (1957).
[3] G. J. Wolga and M. W. P. Strandberg, J. Phys. Chem. Solids 9, 309 (1959).
[4] W. T. Doyle and W. L. Williams, Phys. Rev. Letters 6, 537 (1961).
[5] H. C. Wolf and K. H. Hausser, Naturwissenschaften 46, 646 (1959).
[6] F. H. Hughes and J. G. Allard, Phys. Rev. 125, 173 (1962).

[7] W. C. Holton and H. Blum, Phys. Rev. 125, 89 (1962).
[8] W. L. Williams, Phys. Rev. 125, 82 (1962).
[9] Y. W. Kim, R. Kaplan, and P. J. Bray, Phys. Rev. Letters 6, 4 (1961).
[10] W. C. Holton, H. Blum, and C. P. Slichter, Phys. Rev. Letters 5, 197 (1960).
[11] G. Feher, Phys. Rev. 105, 1122 (1957).
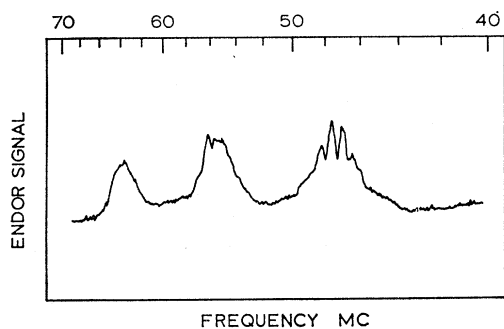[12] N. Lord, Phys. Rev. Letters 1, 170 (1958).

FIG. 1. First- and second-shell ENDOR spectrum. Some second-order splitting is discernible in the low-frequency first-shell line near 48 Mc/sec. In this and in the following figures, the ENDOR signal is the ENDOR induced change in the imaginary part of the susceptibility, $\Delta\chi''$. It appears at the amplitude modulation frequency of the ENDOR oscillator. The angle between a [100] crystal axis and the external magnetic field direction $\theta_H = 0°$.

enough to permit exceptional resolution of the resulting rather fine grained spectrum. In contrast with LiF, even powdered samples of NaH exhibit a well-resolved nineteen-line EPR spectrum.[4,8] ENDOR studies in powdered[13] NaH have confirmed that the resolved EPR pattern is due to the first-shell interaction alone, the other shells contributing only to the width of the individual lines. Because of the isotropic mixture of natural Rb and the high spins of Rb[85] and Cs[133], one would not expect nineteen-line spectra in RbCl and CsCl, even though, as has been established by ENDOR for RbCl,[14] the first-shell interaction predominates. Although powdered samples of NaF do show an EPR spectrum with unimpaired resolution, we shall show here that in NaF the structure is not the expected, and often reported, first-shell pattern. NaH is, thus, the only crystal known to exhibit the characteristic nineteen-line F-center spectrum. In the present paper detailed ENDOR results obtained with single crystals will be presented and related to the resolved EPR spectra observed with both single crystal and powder samples of NaF.

II. EXPERIMENTAL METHODS

The NaF single crystals used in this work were obtained from Semi-Elements, Inc. The powder studies were carried out on analytical reagent NaF obtained from a variety of sources. The samples were x irradiated in a Norelco high-intensity source at 50 kV and 40 mA at a distance of a few centimeters from the target. Although observable EPR signals could be obtained after some minutes of irradiation, it was only after prolonged exposures that satisfactory EPR and ENDOR data were obtained. ENDOR runs were made

at liquid-helium temperature after cumulative irradiations of approximately 10-, 20-, 40-, 60-, and 100-h duration. The only difference noted was a continually improving signal-to-noise ratio. The results reported here are based primarily upon analysis of the long exposure runs. It seems to be considerably harder in NaF than in other alkali halides to get F-center concentrations suitable for EPR and ENDOR studies. This is doubtless one reason why it has been comparatively difficult to obtain satisfactory results in the past with this material.

An X-band superheterodyne magic tee bridge spectrometer, described elsewhere,[13] was used for both the EPR and ENDOR studies. The microwave frequency was 9050 kMc/sec corresponding to resonant magnetic fields of about 3200 G. All observations were made at a temperature of 1.25°K. For the ENDOR work narrow banding was achieved by amplitude modulation of the ENDOR power[15] in place of field modulation of the saturated EPR line.

III. THEORETICAL MODEL

In analyzing the present experimental results the simplest Hamiltonian will suffice. Following Feher[11] we assume that the F-center electron is coupled with individual nuclei through an axially symmetric electron-nuclear magnetic hyperfine interaction. Electric quadrupole interactions,[11] and the finer spectral details that appear when a higher order perturbation calculation is made,[16] can be neglected here. The magnitude of the
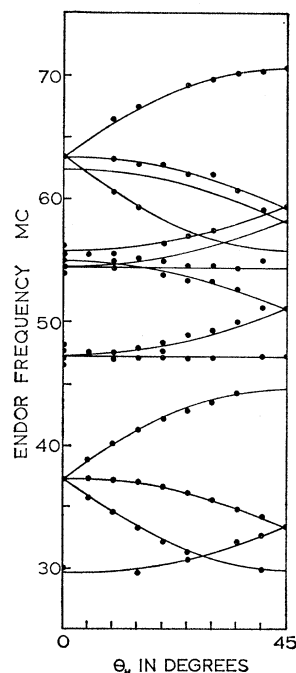

FIG. 2. Angular dependence of the first- and second-shell ENDOR spectra. Both sets of transitions are displayed and were used in obtaining the hyperfine interaction constants given in Table II.

[13] W. T. Doyle, Phys. Rev. 126, 1421 (1962).
[14] H. Seidel and H. C. Wolf, Program of the International Symposium on Color Centers in Alkali Halides, II. Physikalisches Institut der Technischen Hochschule, Stuttgart, Germany, 1962, paper D8, p. 20 (unpublished).

[15] W. T. Doyle, Rev. Sci. Instr. 33, 118 (1962).
[16] T. E. Feuchtwang, Phys. Rev. 126, 1628 (1962).

effects and the resolution of the currently available spectra do not justify their inclusion. The use of an axially symmetric Hamiltonian, often unjustified,[13,17,18] also proves adequate to represent the present observations on NaF.

Within these limitations the ENDOR transition frequencies, $h\nu_{\text{ENDOR}}$, are given by[11]

$$h\nu_{\text{ENDOR}} = \pm g_I \beta_I H + a/2 + (b/2)(3 \cos^2\alpha - 1), \quad (1)$$

where g_I is the nuclear spectroscopic splitting factor, β_I is the nuclear magneton, H is the applied magnetic field, a and b are the isotropic and anisotropic hyperfine interaction constants, respectively, and α is the angle between the axis of symmetry of the anisotropic part of the interaction and the external magnetic field. It is assumed that identical relations hold independently for each nucleus surrounding the F center. These surrounding nuclei may be grouped into crystallographically equivalent shells having identical hyperfine interaction constants. Within a given shell the nuclei may be nonequivalent with respect to orientation. It has become customary to assign to each shell a number, N, equal to the sum of the squares of the reduced nuclear coordinates of a nucleus in that shell relative to the center of the vacancy.[12] This convenient practice has shortcomings, e.g., there is no seventh shell in this numbering scheme, and, beyond the eighth shell the designation is not unique. Thus, there are two kinds of ninth shell. Where ambiguity exists, and, in general, to emphasize the direction in which the nuclei in a given shell lie, we shall have occasion to refer to the shells by the reduced nuclear coordinates, (u, v, w), themselves.

The experimental ENDOR spectra will be analyzed to obtain isotropic and anisotropic interaction constants for the various nuclear shells N. Proper identification of the nuclear species responsible for a given set of lines is insured if use is made of the fact that there are two ENDOR lines for each nucleus, corresponding to the two choices of sign of the first term in Eq. (1). When this term is smaller than the other two, one obtains two identical spectra separated by twice the nuclear magnetic resonance (NMR) frequency for the nucleus involved. When the first term is larger, one obtains two mirror-image spectra bracketing the characteristic
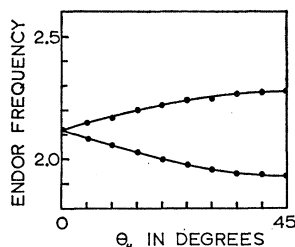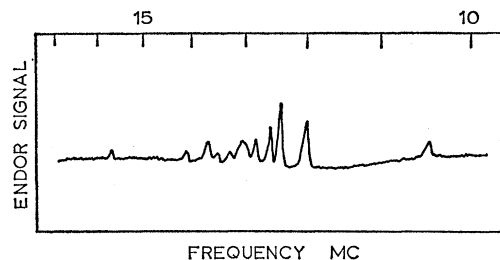

FIG. 4. ENDOR lines due to the fluorine shells from 4 out, for $\theta_H = 0°$. Two mirror-image spectra bracketing the F^{19} NMR frequency at about 13.0 Mc/sec are observed. The outermost lines are due to shell 4. Two other shell 4 lines lie out beyond this frequency range. Other lines due to shells 6, 8, and possibly 16, are also clearly resolved.

NMR frequency. In either case, the type of nucleus may be unambiguously identified from the pattern.[19] It is also essential to observe both sets of transitions to avoid an ambiguity in the evaluation of the isotropic constant, a. Finally, it is important to observe the angular dependence of the ENDOR spectrum over a wide range of α. When, as is usually the case, rotation about a [100] crystal axis is employed, the angle between the external magnetic field and a second [100] crystal axis, θ_H, should be varied over the full range from 0° to 45° (preferably over a larger range) to insure a correct shell assignment from the symmetry of the pattern. This is especially important for the outer shells, where the magnitude of the isotropic constant is an unreliable guide to shell assignment and the contributions of many different shells cluster about the NMR frequency, overlapping badly. As far as possible, these precautions have been observed with all the spectra to be reported here. In a few cases involving outer shells it was not possible to follow the angular dependence in detail throughout the entire range. These cases will be considered separately below and reasons for the assignments adduced.

The EPR transition frequencies, $h\nu_{\text{EPR}}$, corresponding to the set of isotropic and anisotropic interactions $a(N)$ and $b(N)$ are given by

$$h\nu_{\text{EPR}} = g_J \beta_0 H + \sum_i [a(i) + b(i)(3 \cos^2\alpha - 1)]M_I(i), \quad (2)$$

where the $M_I(i)$ is the magnetic quantum number of the ith nucleus, g_J is the electronic spectroscopic splitting factor, and β_0 is the Bohr magneton. The other quantities are as defined above. The sum is to be extended over all nuclei in all shells. In the most general

FIG. 3. Angular dependence of the low-frequency shell 3 ENDOR spectrum. The high-frequency shell 3 spectrum was also observed.

[17] M. F. Deigen and V. Ia, Zevin, Zh. Eksperim. i Teor. Fiz. **34**, 1142 (1958) [translation: Soviet Phys.—JETP **7**, 790 (1958)].
[18] H. Seidel, Z. Physik **165**, 218 (1961).

[19] This also helps in identifying spurious signals that sometimes appear at subharmonics of the ENDOR frequency. These signals seem to be an experimental artifact due to harmonic generation in wide band amplifiers following the ENDOR rf oscillator, and are better eliminated. These effects may be minimized by avoiding overloading the last amplifying stage or, preferably, by generating the ENDOR power directly with a power oscillator, loop coupling the high Q tank circuit directly to the ENDOR coil in the cavity. This method has been employed by H. Seidel (Ref. 18) and he has never been troubled by spurious subharmonic responses (private communication).
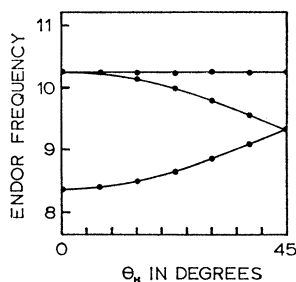
FIG. 5. Angular dependence of the low-frequency shell 4 lines. The upper frequency shell 4 lines were also studied.

case this sum involves a large number of overlapping noncoincident lines, so no resolved structure is observed. Special relations among the various interactions $a(N)$ and $b(N)$ are required for a resolved pattern to occur. Thus, when $a(1)$ is much larger than all other interactions one observes the simple first-shell nineteen-line spectrum predicted by Kip, Kittel, Levy, and Portis[1] and observed in NaH. When $a(1)$, $b(1)$, $a(2)$, and $b(2)$ are all comparable one may still have a resolved spectrum if at certain angles further accidental rela-

TABLE I. Distribution of intensities of the 31 resolved electron paramagnetic resonance lines of the F center in NaF. M_I is the total nuclear magnetic quantum number of the first two shells and W is the weight of the corresponding line. The total weight of all lines is $(4096)^2$.

M_I	W
0	2 031 568
±1	1 942 947
±2	1 698 726
±3	1 355 581
±4	984 612
±5	648 267
±6	384 674
±7	204 117
±8	95 832
±9	39 239
±10	13 734
±11	3 993
±12	924
±13	159
±14	18
±15	1

tionships exist, provided that all other constants are very much smaller. This is the situation in LiF, in which a host of very narrow lines are observed at special angles. Still another way in which a resolved pattern can occur arises when $a(1) \approx a(2)$ and the other constants are reasonably small (they need not be very much smaller in this case). This will be shown to be the situation in NaF. Under these conditions one observes a simple isotropic spectrum resembling, at first glance, the nineteen-line pattern of NaH. Now, however, there will be more than nineteen lines. A total of $2[6I(1) + 12I(2)] + 1$ lines appear, where $I(1)$ and $I(2)$ are the spins of the first- and second-shell nuclei, respectively. For NaF (with first- and second-shell spins of $\frac{3}{2}$ and $\frac{1}{2}$, respectively) a 31-line pattern is expected. In NaF the first-shell interaction may be thought of as producing

the nineteen-line pattern in the usual way, the second-shell interaction, in turn, splitting each of the nineteen lines into groups with identical spacings. Provided that $a(1) \approx a(2)$, all of the nineteen groups of lines will be in register. There is then no loss of resolution even in powders, but twelve additional lines appear. The over-all distribution of intensities is given in Table I. The width of the individual components depends upon the accuracy of the coincidence of the first- and second-shell interactions, as well as upon the magnitude of all of the other $a(N)$ and all of the $b(N)$. Nothing definite can be learned from the apparent resolution of the EPR pattern in this case.

IV. EXPERIMENTAL RESULTS AND DISCUSSION

Since the results and interpretation to be presented are in conflict with all previous work on NaF, they will be presented in detail. The ENDOR spectra due to the first two shells are shown in Fig. 1, for $\theta_H = 0$. The lines are very broad and weak, so the signal-to-noise ratio leaves much to be desired. This is not peculiar to this particular sample, which was heavily colored, and it probably explains why an earlier attempt to observe these lines[7] was unsuccessful. The extraordinary breadth of these inhomogeneously broadened lines is due to quadrupolar effects and second-order effects arising from the fact that the F center possesses a center of symmetry.[16] This can be seen in the partially resolved structure of the first-shell low-frequency line near 48 Mc/sec. Poor signal-to-noise ratio and overlapping of spectra precluded a thorough study of these finer effects. The gross angular dependence, however, was observed and is shown in Fig. 2. Reliable hyperfine interactions were readily obtained in spite of overlapping. The anisotropic constants were computed primarily from the low-frequency set of first-shell lines and the high-frequency set of second-shell lines, the remaining lines serving as a check.

Beyond the second shell the interaction of both anion and cation nuclei with the external field is larger than the hyperfine interactions with the center electron. The remaining ENDOR lines due to these outer shells are grouped about the Na^{23} and F^{19} NMR frequencies at 3.6 and 13.0 Mc/sec, respectively. Since shell 3 gives rise to an unambiguous ENDOR spectrum, the actual data are not displayed. Figure 3 shows the angular
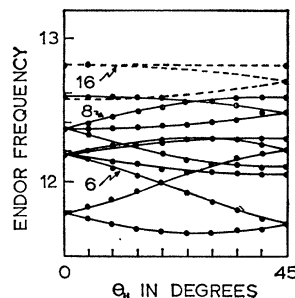

FIG. 6. Angular dependence of the low-frequency ENDOR spectra due to the outer fluorine shells. Shells 6 and 8 are readily recognized. The broken line indicates a poorly resolved component tentatively assigned to shell 16.

dependence observed for this shell. Hyperfine constants were computed using sum and difference frequencies.

The ENDOR lines due to the outer fluorine shells are shown in Fig. 4 for $\theta_H=0$. The sum and difference frequencies appear as mirror images on either side of 13.0 Mc/sec. The outermost lines belong to shell 4. Two other shell 4 lines lie out beyond this frequency range. The angular dependence of shell 4 is shown in Fig. 5. Both sum and difference lines were used to compute the hyperfine constants. All the other fluorine shell lines overlap to some extent, so it is preferable to display the angular dependence of the entire set together in Fig. 6. Fluorine shells 6 and 8 are immediately recognized by their characteristic patterns and are so labeled in the figure. Other lines very close to the fluorine NMR frequency were also partially resolved. The angular dependence could not be followed in detail, but from the pattern near 0° and 45° they could be due to shell 16 or, possibly shell 10, but not shells 12 or 14. They are tentatively assigned to shell 16.

The resolution of the angular dependence of the outer fluorine lines is not equalled in the outer sodium shells beyond shell 3, primarily because of the very large number of overlapping lines. The difference frequency ENDOR spectrum due to these ions is shown in Fig. 7 for $\theta_H=0$. A weaker mirror image sum frequency pattern was also observed. This pattern contains contributions due to all of the cation shells from 5 out. In this orientation one observes a rather unusual spectrum. A group of six strong lines (numbered 1-6 in Fig. 7) separated by a distinct gap from a weaker, and presumably composite, line closely bracketing the sodium NMR frequency. Considering first the set of six stronger lines, it is clear that shells beyond the fifth are involved, since shell 5 alone would give rise to only three lines in this orientation. Actually the intensity and shape of line 1 show that it must be due to a superposition of lines, and this is borne out by studies of the angular dependence.

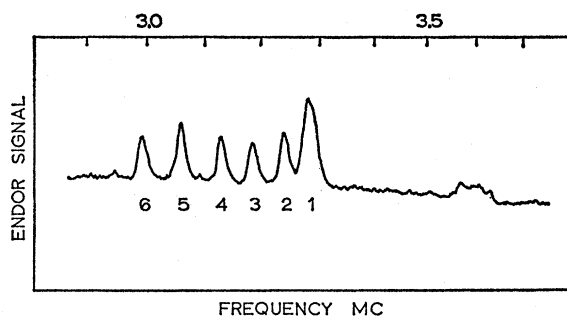The angular dependence of this group of lines was

FREQUENCY MC

FIG. 7. Low-frequency ENDOR spectra due to the outer sodium shells from 5 out, for $\theta_H=0°$. The presence of six strong lines, numbered 1-6, clearly indicates a contribution from cation shells beyond 5. The strong lines are attributed to shells 5, 9A, and 13 (see text). Still other shells are responsible for the composite line near the Na[23] NMR frequency at about 3.6 Mc/sec.

FIG. 8. Angular dependence of the low-frequency ENDOR lines due to the outer cation shells from 5 out. The spectrum is difficult to follow beyond about 15°. The lines drawn are consistent with assignments to shells 5, 9A, and 13 as discussed in the text. They must be considered merely schematic at the larger angles. The vertical lines indicate the presence of broad regions of absorption due, presumably, to overlapping of lines. The numbers indicated near $\theta_H=0°$ identify the corresponding peaks in Fig. 7.
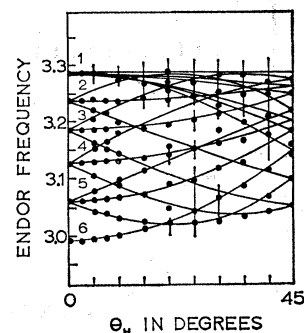
hard to follow due to the particularly severe overlapping of spectra. Caution is required in interpreting the angular dependence. It would be misleading to decompose this rather tangled set of lines in a procrustean manner and display the angular dependence separately

TABLE II. Experimental values of the magnetic hyperfine interaction constants in Mc/sec for *F* centers in NaF. Here $a(N)$ is the isotropic contact term for the *N*th shell and $b(N)$ is the corresponding anisotropic term. The shell number is the sum of the squares of the reduced nuclear coordinates. Shells 7 and 15 do not exist. For simplicity axial symmetry about the line joining the nucleus and the center of the vacancy is assumed for all shells, regardless of the symmetry of the site. Experimental uncertainty is in the last digit quoted.

Shell	Ion	Direction	$a(N)$ Mc/sec	$b(N)$ Mc/sec
1	Na[23]	[001]	107.0	5.3_0
			(220)[a]	(5.4)[a]
2	F[19]	[011]	96.8	9.8_0
3	Na[23]	[111]	3.0_7	0.3_4
4	F[19]	[002]	6.5_3	1.2_7
5	Na[23]	[012]	0.7_6	0.2_1
6	F[19]	[112]	1.5_3	0.5_4
8	Na[23]	[022]	0.7_3	0.3_2
9A	F[19]	[003]	0.8_0	0.2_0
9B	F[19]	[122]		
10	Na[23]	[013]		
11	F[19]	[113]		
12	Na[23]	[222]		
13	F[19]	[023]	0.7_6	0.1_6
14	Na[23]	[123]		
16	F[19]	[004]	0.1_2[b]	0.1_5[b]

[a] See Ref. 25.
[b] Tentative assignment (see text).

according to an assumed shell assignment. The more so since these same lines were assigned in a different way by Holton and Blum in their earlier ENDOR experiment.[7] The angular dependence of the entire set is shown in Fig. 8. The lines drawn are consistent with the shell assignments to be made here and require some explanation. It is difficult to follow the lines as they cross and recross beyond about 15°. Beyond 15° the lines drawn must be considered merely schematic. Nevertheless, shell assignments may be made with some confidence on the basis of the angular dependence near $\theta_H=0°$ in the following way. Lines 5, 2, and part of 1 in Fig. 8 are assigned to shell 5. They have the proper
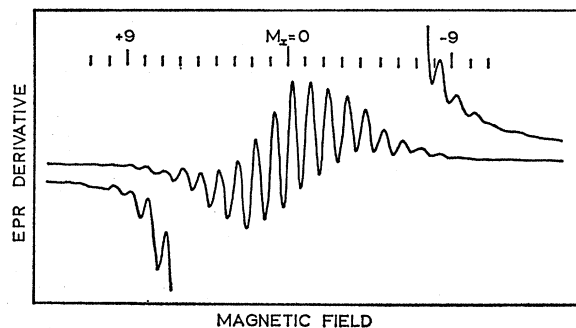
FIG. 9. Resolved EPR spectrum in NaF. The near equality of the first- and second-shell isotropic hyperfine interaction leads to a predicted 31-line resolved pattern. The outer portions of the spectrum were retraced with the gain increased by 10. Several additional lines beyond the previously reported 19 may be seen.

spacing and angular dependence near zero, and, to a fair extent, may be followed over the entire range of angles. This assignment is relatively straightforward and, once made, simplifies the interpretation of the rest of the pattern. Hyperfine interactions for shell 5 were computed assuming axial symmetry about the line joining the center of the vacancy and the shell 5 nuclei, even though the symmetry of the site does not demand this. Seidel[18] has shown that departures from axial symmetry in shell 5 are of the order of 7% in NaCl and the axis of symmetry departs by 9° from the 210 direction. These corrections are neglected here, both in shell 5 and in other shells where similar small departures might be expected.

Line 6 can only be the outer line of a shell having the same symmetry as shell 1. It may, thus, be assigned to shell 9. From the angular dependence of this outer line the other ninth shell line expected at 0° would lie under peak 1. This is consistent with the strength of the peak. It may be noted that shell 9 is one for which the shell number alone is ambiguous. The nuclei responsible for lines 6 and 1 lie at positions (003) in the ninth shell (shell 9A). Other nuclei at positions (122) also lie at the same distance from the center of the vacancy in another type of ninth shell (shell 9B). No trace of these shell 9B nuclei at (122) was found.

More difficulty was encountered in the assignment of lines 3 and 4 of Fig. 7. As can be seen in Fig. 8, both of these lines split very rapidly into triplets in the neighborhood of $\theta_H = 0°$. This behavior is incompatible with the symmetry of shells 9B, 11, 17, and a number of higher cation shells. There is no shell 15. Shell 13, however, does have a pair of levels that split into identical triplets near 0° as lines 3 and 4 do in Fig. 8. The other shell 13 line that appears at 0° must again be assumed to lie under line 1. Line 1 has thus been forced to absorb the "missing" lines of shells 5, 9A, and 13. The area under line 1 is great enough to permit this interpretation, and would be difficult to explain without it. The over-all angular dependence confirms the assignments within the limits of the resolution.

As for the weak cluster of lines near 13.0 Mc/sec, little can be said. The gap between this central group and the 6 strong lines already identified is striking. If, as seems likely, one can rule out very weak intensities and rather peculiar relationships between the hyperfine interaction constants of shells 9B and 11, both between themselves and with those of the lines already identified, such that they could hide without a trace in the group of stronger lines, one can set a limit on the quantity $a+2b$, and a still smaller limit on a itself, for these (and all other) cation shells. It must be bounded by the very small compass of the central group of lines. For all of these shells $a+2b < 0.05$ Mc/sec. In short, we may conclude that an easily measurable electron density is found in shells 9A and 13, while very little, or none, is found in shells 9B and 11. Clearly, the assumption of spherical symmetry is inadequate for these outer shells.

The hyperfine constants for shells 1 through 16 are gathered together in Table II. Although NaF has been studied in the past by both EPR[2,3] and ENDOR,[7] no correspondence between the results in Table II and earlier results can be expected. In the earlier EPR work isotropic interaction constants for the first two shells were computed from the spacing and apparent resolution of the resolved pattern.[2,3] However, the analysis was based on the assumption of a nineteen-line pattern due to the first-shell nuclei alone, the apparent resolution being attributed to the second-shell isotropic interaction. However, as Table II shows, the first- and second-shell isotropic constants are almost equal. The observed spacing in the resolved pattern is, thus, a kind of weighted mean spacing for the first two shells. Further, it is clear that nothing can be learned of the second shell isotropic interaction from the widths of the resolved lines, since this is already contributing to the splitting of the lines. The apparent resolution of the pattern actually arises from a wide variety of residual affects, e.g., nonidentity of the first- and second-shell isotropic constants, second-order corrections to the Breit-Rabi equation,[20] nonzero first- and second-shell anisotropic interactions, and comparable outer shell interactions. All that can be said is that the apparent resolution of the EPR spectrum seems to be in rough accord with the widths expected from these residual effects.

Because the near equality of the first- and second-shell isotropic interactions leads one to expect a 31-line rather than a 19-line pattern, a search was made for additional lines. Figure 9 shows the EPR derivative spectrum observed with NaF at 1.25°K. The spectrum was first traced through under low gain to keep the recorder on scale throughout the spectrum. Then the gain was increased by a factor of 10 and the spectrum was retraced. During the high-gain run the recorder was turned off in the central part of the spectrum to

[20] G. Breit and I. Rabi, Phys. Rev. 38, 2082 (1931).

protect it. The resultant curves are superposed in Fig. 9. Under high gain several additional lines may be seen out beyond the inner nineteen. The signal-to-noise ratio was very favorable and in other runs still higher gains were used, without however, uncovering further resolved lines. An extended effort was not made to see all of the predicted 31 lines, since it suffices to show that some lines beyond the 19 exist. Moreover, as can be seen in Table I, the outermost lines will be down in intensity from the middle line by a factor of over 2×10^6. Actually, the hope of seeing the outermost lines is even more forlorn, since the presence of anisotropic terms and the lack of exact equality between the first- and second-shell isotropic constants will both produce a smearing of the pattern which become relatively worse in the outer lines. Some evidence for the presence of the outermost lines is seen in the gradual smooth rise in the EPR derivative curve out beyond the 23 resolved lines. The distribution of intensities of the resolved lines is roughly Gaussian and is consistent with those given in Table I, within the limits expected in view of the residual effects. The relative smallness of the anisotropic terms listed in Table II insures near isotropy of the resolved EPR spectrum. In a single crystal with $\theta_H = 0°$, and in a powder, the contribution of the first-shell nuclei at $90°$ and the second-shell nuclei at $45°$ dominate the pattern. As it happens the quantity $a/2 + b/2 (\cos^2\alpha - 1)$ is almost exactly equal for these two groups of nuclei. Since the anisotropic terms are small, exact equality would not be required, but it probably improves the resolution. It also accounts for the very close agreement for the splitting in the single crystal and powder spectra.

The hyperfine interactions obtained for NaF by Holton and Blum[7] are also in disagreement with the results reported here. They were unable to observe the ENDOR spectra due to shells 1 and 2. However, they computed isotropic interaction constants for the first two shells from the resolved EPR spectrum. Although they do not report in detail how they obtained these constants, it seems likely that their values are in error, at least in part, because of neglect of anisotropic terms and to assignment of the dominant splitting to the first-shell nuclei alone. Holton and Blum also reported hyperfine interaction constants for shells 3 through 8 based upon ENDOR measurements. These values are also in error, presumably because they also failed to see shells 3 and 4, and, as a result, were forced into misinterpreting the ENDOR lines that they did see. It is easy to appreciate how this could happen considering the great degree of overlapping of the outer shell lines and the relative weakness of the entire ENDOR pattern.

No effort was made to compute an accurate g value. The second order correction to the Breit-Rabi equation is quite large for such a widely split line, and to apply it in NaF would require an elaborate computer fitting procedure. Indeed, there does not even seem to be

agreement, in principle, on how to apply this correction to the *F* center.[2,3,6,21] Without the correction the experimental uncorrected g value, which as usual is close to 2, lacks theoretical significance. Earlier reported g values[2,3] must be regarded skeptically on three counts: A variety of second-order corrections have been applied, they have been applied assuming a nineteen line spectrum, and the published spectra have been strongly contaminated with an impurity signal in the center of the line. This impurity signal appears in the initial stages of coloration in NaF. It is not noticeable in Fig. 9, but this is a heavily colored specimen.

For many purposes the *F*-center wave function may be pictured as a comparatively slowly varying function of position between the ions, joining smoothly to rapidly varying atom-like wave functions inside the individual ion cores. This basic conception has been a common feature of a number of *F*-center calculations. For some purposes the rapid variations may be ignored to a first approximation. For the isotropic hyperfine interaction calculations it is, of course, crucial to include the intracellular oscillations. Several prescriptions, differing in detail, but basically similar, have been given for bringing the intracellular oscillations into this picture.[22-24] Among these the point-ion-lattice model of Gourary and Adrian[24] is particularly attractive, because it has the conceptual advantage of a well-defined general procedure. A characteristic feature of the Gourary and Adrian method is the orthogonalization of a smooth "envelope function" to the ion cores orbitals. This, in effect, makes the *F*-center wave function look much like the atomic wave functions near the nuclei while joining them smoothly together between the ions without the introduction of *ad hoc* methods. Many simplifying assumptions are required in order to carry out the calculations in a practical case. Among these, the neglect of lattice distortions, exchange, overlap, the influence of the high-frequency dielectric constant, and the assumption of a spherically symmetric potential may be mentioned. Although the items in the list are neither mutually independent nor exhaustive, they probably account for most, if not all, of the current discrepancies between theory and experiment. Some of the neglected effects are particularly in evidence in NaF.

Although the theory of the hyperfine interactions in NaF is not yet highly developed, this crystal deserves further detailed theoretical study. The wave functions of both ions are known and fairly compact. At present, theoretical values, due to Adrian, Blumberg, and Das,[25] are available for the first-shell constants $a(1)$ and $b(1)$.

[21] W. B. Lewis and F. E. Pretzel, J. Phys. Chem. Solids 19, 139 (1961).
[22] D. L. Dexter, Phys. Rev. 93, 244 (1954).
[23] J. A. Krumhansl, Phys. Rev. 93, 245 (1954).
[24] B. S. Gourary and F. J. Adrian, in *Solid State Physics*, edited by F. Seitz and D. Turnbull (Academic Press Inc., New York, 1960), Vol. 10, p. 127.
[25] F. J. Adrian, W. E. Blumberg, and T. P. Das, quoted in Ref. 24, p. 223.

These are tabulated in brackets in Table II. As usual in current calculations based on the point-ion-lattice model the isotropic interactions are too high by about a factor of 2. This could be due to neglect of exchange effects, as suggested by Gourary and Adrian,[24] or to neglect of core polarization; probably both. The calculated anisotropic constant, on the other hand, is in excellent agreement with experiment, although exact agreement is doubtless fortuituous.

The radial dependence also departs measurably from the predictions of the point-ion-lattice model. In common with other alkali halides for which contributions from a number of shells have been observed,[7,18] the wave function falls off more slowly with distance than expected. This is particularly noticeable here for ions lying along the [100] direction. There is a contribution from shell 9A at [003], but none from shell 9B at [122], although both shells have the same radius. Similarly, anion shell 13 at [023] is present, while shell 11 at [113], nearer the vacancy, is not. Finally, though less certainly, shell 16 at [004] seems to be present while shells 10, 12, and 14 do not. Qualitatively, this can be viewed as a focusing of the wave function along atom-rich directions and planes, particularly, in the [001] and [011] directions. The way in which this effect manifests itself theoretically depends upon the calculational method employed. It would arise naturally as an overlap effect in a straightforward LCAO type calculation. It could presumably be built into more elaborate calculations using the point-ion-lattice approach as well. For the outer reaches of the wave function the effect can even be regarded as a manifestation of an anisotropic effective mass.

At present the agreement between theory and experiment may be considered satisfactory, considering the great difficulties encountered in the theory. The experiments, on the other hand, are very easy to perform and they yield much detailed information. They can provide a valuable, and probably indispensible, guidance in future theoretical calculations.

The question of the nature of the M center has been widely studied in recent years. Many vain attempts have been made to observe a paramagnetism which could be identified with M centers. Recently, Holcomb[26] and Blum[27] have called attention to the fact that NaF

is well suited for this kind of search. A relatively large M band can be obtained in NaF, and the well resolved and characteristic F-center EPR spectrum make it unlikely that an M-center EPR signal would be undetected or confused with exchange narrowing effects. Neither Holcomb nor Blum found evidence for a paramagnetic M center using EPR. Our samples also contained large concentrations of M centers, but again no evidence of their presence was observed in the resolved EPR spectrum. Moreover, the ENDOR method, which is a more powerful aid in a search of this kind, also gave no evidence of the presence of M centers. The ENDOR technique permits this search to be made just as readily in crystals displaying unresolved or partially resolved spectra. We have made an extensive, but fruitless, effort to see ENDOR evidence of M centers in a number of crystals. In one sample of LiF the M band itself made the crystal so black that even the thinnest samples were unsuitable for optical measurements, yet no trace of additional ENDOR lines was found. In the same sample the F-center ENDOR lines had a signal-to-noise ratio too large to be measured reliably. This evidence in favor of an electron-paired M center seems overwhelming. A result that is perhaps not unexpected on chemical grounds.

V. CONCLUSION

It has been shown that the resolved EPR spectrum in NaF arises from the chance equality of the first- and second-shell isotropic hyperfine interaction constants. ENDOR spectra have been observed for nuclei out to the sixteenth shell. The dependence of the isotropic interaction upon distance from the center departs appreciably from the predictions of the point-ion-lattice model. In particular, the F-center wave function departs from spherical symmetry. Along certain directions, such as [100], the wave function extends deep into the surrounding crystal. The observations indicate the need to include overlap effects into future calculations. An extensive search for M center ENDOR lines was unsuccessful, even though a strong optical M band was present in the crystals.

ACKNOWLEDGMENTS

[26] D. F. Holcomb, Program of the International Symposium on Color Centers in Alkali Halides, II. Physikalisches Institut der Technischen Hochschule, Stuttgart, Germany, 1962, paper D2, p. 17 (unpublished).

[27] H. Blum, Phys. Rev. 128, 627 (1962).